

Modular Model-Based Bayesian Learning for Uncertainty-Aware and Reliable Deep MIMO Receivers

Tomer Raviv, Sangwoo Park, Osvaldo Simeone, and Nir Shlezinger

Abstract—In the design of wireless receivers, deep neural networks (DNNs) can be combined with traditional model-based receiver algorithms to realize modular hybrid model-based/data-driven architectures that can account for domain knowledge. Such architectures typically include multiple modules, each carrying out a different functionality. Conventionally trained DNN-based modules are known to produce poorly calibrated, typically overconfident, decisions. This implies that an incorrect decision may propagate through the architecture without any indication of its insufficient accuracy. To address this problem, we present a novel combination of Bayesian learning with hybrid model-based/data-driven architectures for wireless receiver design. The proposed methodology, referred to as *modular model-based Bayesian learning*, results in better calibrated modules, improving accuracy and calibration of the overall receiver. We demonstrate this approach for the recently proposed DeepSIC multiple-input multiple-output receiver, showing significant improvements with respect to the state-of-the-art learning methods.

I. INTRODUCTION

The capacity of deep neural networks (DNNs) to learn complex tasks from data has led to a burgeoning interest in their utilization for communications receiver design [1]–[5]. Traditional receiver algorithms based on the mathematical modeling of signal transmission, propagation, and reception, are seemingly being supplanted by DNN-based receivers, which can operate efficiently in scenarios where the channel model is unknown, highly complex, or difficult to optimize [4]. DNN-aided receivers are often envisioned to be important contributors to meeting the rapidly increasing demands in throughput, coverage, and robustness [6].

Despite the much touted potential of DNNs-aided receivers [7], their deployment faces several challenges that may limit their direct applicability to communications. In fact, wireless communication is fundamentally distinct from conventional deep learning domains, such as computer vision and natural language processing [8], owing to the dynamic nature of wireless channels. Consequently, the training algorithms have limited data corresponding to any given channel realization.

T. Raviv and N. Shlezinger are with the School of ECE, Ben-Gurion University of the Negev, Beer-Sheva, Israel (e-mail: tomerraviv95@gmail.com, nirshl@bgu.ac.il). S. Park and O. Simeone are with KCLIP lab at the Department of Engineering, King’s College London, U.K. (email: {sangwoo.park; osvaldo.simeone}@kcl.ac.uk). The work of T. Raviv and N. Shlezinger was partially supported by the Israeli 5G-WIN consortium. The work of S. Park and O. Simeone was partially supported by the European Research Council (ERC) under the European Union’s Horizon 2020 Research and Innovation Programme (grant agreement No. 725732). The work of O. Simeone was also supported by the European Union’s Horizon Europe project CENTRIC (101096379), and by an Open Fellowship of the EPSRC (EP/W024101/1).

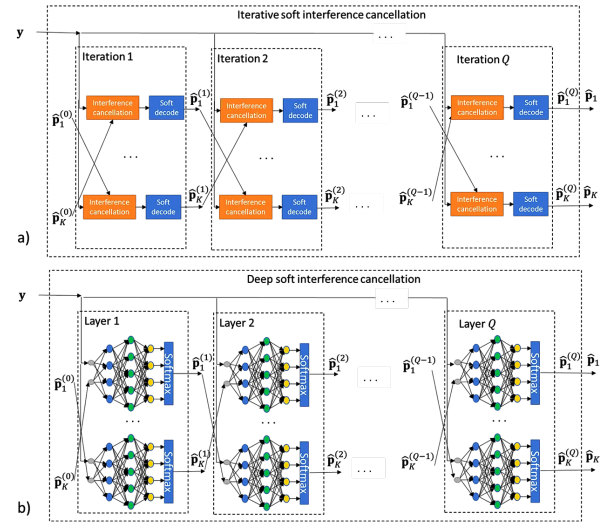


Fig. 1: (a) Iterative SIC; and (b) DeepSIC [12]. In this paper, we introduce modular model-based Bayesian learning, which calibrates the internal modules of the DeepSIC architecture with the double goal of improving end-to-end accuracy and of producing well-calibrated soft outputs for the benefit of downstream tasks.

Under such conditions, conventionally trained DNNs are prone to overfitting [9], and are likely to produce wrong decisions with high confidence, i.e., to yield poorly calibrated outputs [10], [11].

Various approaches have been proposed to enhance the performance and calibration of DNN-aided receivers in the presence of limited data. A prominent approach is to incorporate model-based receiver algorithms into a *modular hybrid model-based/data-driven architecture* [13], [14]. Such architectures present separate modules [15], with each module carrying out a specific functionality within the receiver processing chain. Modularity facilitates the use of available domain knowledge, reducing the number of free parameters as compared to conventional black-box DNNs, and enhancing the generalization capability of DNN-based receivers [12], [16]–[20].

Despite the improved sample efficiency, hybrid model-based/data-driven architectures may be negatively affected by the inclusion of conventionally trained DNN-based modules, which are known to produce poorly calibrated, typically *overconfident*, decisions. Poorly calibrated DNN-based modules

may propagate inaccurate predictions through the architecture without any indication of their insufficient accuracy.

A principled approach to improve calibration relies on the adoption of *Bayesian learning* [11], [21]–[23], which treats the parameters of DNNs as random variables. This allows Bayesian learning to account for the *epistemic* uncertainty that arises due to lack of training data. Bayesian learning was shown to improve the reliability of DNNs in wireless communication systems [24], [25]. Nonetheless, these existing studies adopt *black-box* architectures, and are hence not applicable to modular model-based/data-driven receivers.

Our work presents a novel methodology, referred to as *modular model-based Bayesian learning*, that combines Bayesian learning with hybrid model-based/data-driven architectures. The proposed approach calibrates the internal DNN-based modules, rather than merely calibrating the overall system output. By doing so, the proposed modular model-based Bayesian learning ensures a reliable interplay between the modules. This has the double advantage of improving end-to-end accuracy and yielding well-calibrated soft outputs that can benefit downstream tasks.

Our main contributions are summarized as follows:

- **Modular model-based Bayesian learning:** We introduce a modular model-based Bayesian learning framework that integrates Bayesian learning with model-based deep learning. Accounting for the modular architecture of hybrid model-based/data-driven receivers, Bayesian learning is applied on a per-module basis. The approach is exemplified and detailed for the DeepSIC multiple-input multiple-output (MIMO) receiver introduced in [12].
- **Extensive experimentation:** We evaluate the advantages of modular model-based Bayesian learning for deep MIMO receivers in terms of bit error rate (BER) and calibration performance of the demodulator. The proposed model-based Bayesian DeepSIC outperforms the conventional frequentist DeepSIC, as well black-box solutions, over a wide range of signal-to-noise ratios (SNRs). Furthermore, the final soft outputs produced by the proposed approach are shown to be better calibrated than both frequentist and standard Bayesian learning.

Throughout the paper, we use boldface letters for vectors, e.g., \mathbf{x} . Upper-cased boldface letters denote matrices, e.g., \mathbf{X} . Calligraphic letters, such as \mathcal{X} , are used for sets, with $|\mathcal{X}|$ being the cardinality of \mathcal{X} , and \mathcal{R} the set of real numbers.

II. SYSTEM MODEL AND PRELIMINARIES

In this section, we describe the MIMO communication system under study in Subsection II-A, and we review the conventional frequentist learning of MIMO detectors in Subsection II-B. We then briefly present basics of Bayesian learning for deep receivers in Subsection II-C; and model-based deep receivers in Subsection II-D, focusing on DeepSIC [12].

A. System Model

Consider an uplink MIMO digital communication system with K single-antenna transmitters (users). The users transmit

messages, independently of each other, to a receiver (base station) with N antennas. At time index i , each k^{th} user generates its transmitted symbol $s_k[i]$ from the set of constellation points \mathcal{S} , forming the $K \times 1$ transmitted vector $\mathbf{s}[i] \in \mathcal{S}^K$ of the K different users. The corresponding received signal vector $\mathbf{y}[i] \in \mathcal{R}^N$ is generally determined as

$$\mathbf{y}[i] \sim P_{\mathbf{h}}(\mathbf{y}[i]|\mathbf{s}[i]), \quad (1)$$

which is subject to the unknown conditional distribution $P_{\mathbf{h}}(\cdot|\cdot)$ that depends on the current channel parameters \mathbf{h} .

We adopt a block-fading model, where the channel \mathbf{h} is constant within a block of duration dictated by the coherence of the channel. Denoting the size of this block as B^{tran} symbols, a single block is generally divided into two parts: The first composed of B^{pilot} pilots and the other of $B^{\text{info}} = B - B^{\text{pilot}}$ information symbols. Hence, the corresponding indices for transmitted pilot symbols and information symbols can be written as $\mathcal{B}^{\text{pilot}} = \{1, \dots, B^{\text{pilot}}\}$, and $\mathcal{B}^{\text{info}} = \{B^{\text{pilot}} + 1, \dots, B^{\text{tran}}\}$, respectively.

B. Frequentist DNN-Aided Receivers

DNN-aided receivers learn to map the channel outputs \mathbf{y} into corresponding transmitted symbols s . Specifically, DNN-aided receivers output a conditional probability distribution on the symbols given the channel output that is parameterized by trainable weight vector φ . The resulting probabilistic output for a channel output $\mathbf{y}[i]$ is denoted as $\{P_{\varphi}(s|\mathbf{y}[i])\}_{s \in \mathcal{S}^K}$.

In conventional *frequentist* learning, optimization of the parameter vector φ is done by minimizing the cross-entropy loss using the labeled pilots [2], i.e.,

$$\varphi^{\text{freq}} = \arg \min_{\varphi} \mathcal{L}_{\text{CE}}(\varphi), \quad (2)$$

with $\mathcal{L}_{\text{CE}}(\varphi)$ defined as

$$\mathcal{L}_{\text{CE}}(\varphi) = - \sum_{i \in \mathcal{B}^{\text{pilot}}} \log P_{\varphi}(s[i]|\mathbf{y}[i]). \quad (3)$$

After optimization, the trained receiver is used to detect information symbols as

$$\hat{s}[i] = \arg \max_{s' \in \mathcal{S}^K} P_{\varphi^{\text{freq}}}(s'|\mathbf{y}[i]), \quad \forall i \in \mathcal{B}^{\text{info}}. \quad (4)$$

In the presence of limited data, the conventional receiver in (4) tends to suffer from overfitting when the number of parameters (the cardinality of φ) is large. This may cause a degraded accuracy, i.e., a high probability that $\hat{s}[i] \neq s[i]$, at test time. Furthermore, the trained receiver (4) tends to produce overconfident predictions. This is in the sense that the confidence level $P_{\varphi^{\text{freq}}}(\hat{s}[i]|\mathbf{y}[i])$ produced by the receiver is typically larger than the actual test accuracy of the decisions. Overfitting can be alleviated via the adoption of hybrid model-based deep receivers, while poor calibration can be addressed via Bayesian learning. We next elaborate on these individual approaches, starting with the latter.

Algorithm 1: DeepSIC

Input : Channel output \mathbf{y} ; Parameter vector φ^{SIC} .
Output: Soft estimations for all users $\{\hat{P}^{(k,Q)}\}_{k=1}^K$.

- 1 **DeepSIC Inference**
- 2 Generate an initial guess $\{\hat{P}^{(k,0)}\}_{k=1}^K$.
- 3 **for** $q \in \{1, \dots, Q\}$ **do**
- 4 **for** $k \in \{1, \dots, K\}$ **do**
- 5 $\hat{P}^{(k,q)} = P_{\varphi^{k,q}}(\cdot | \mathbf{y}, \{\hat{P}^{(l,q-1)}\}_{l \neq k})$;
- 6 **return** $\{\hat{P}^{(k,Q)}\}_{k=1}^K$

C. Bayesian Learning

Bayesian learning treats the model parameter vector φ as a *random vector* obeying a distribution $p^b(\varphi)$ that accounts for the available data and for prior knowledge. Specifically, the distribution is obtained by minimizing the *free energy loss*, also known as negative evidence lower bound (ELBO) [11],

$$p^b(\varphi) = \arg \min_{p'} \left(\mathbb{E}_{\varphi \sim p'(\varphi)} [\mathcal{L}_{CE}(\varphi)] + \frac{1}{\beta} \text{KL}(p'(\varphi) \| p^{\text{prior}}(\varphi)) \right). \quad (5)$$

The Kullback-Leibler (KL) divergence term in (5), $\text{KL}(p'(\varphi) \| p(\varphi)) = \mathbb{E}_{p'(\varphi)} [\log \frac{p'(\varphi)}{p(\varphi)}]$, regularizes the optimization of $p^b(\varphi)$ with a prior distribution $p^{\text{prior}}(\varphi)$; and the hyperparameter $\beta > 0$, known as inverse temperature parameter, balances the regularization impact [9], [11].

Once optimization (5) is carried out, Bayesian learning dictates that the output conditional distribution for the transmitted information symbol be given by the *ensemble* decision

$$P_{\varphi^{\text{Bayes}}}(\mathbf{s}[i] | \mathbf{y}[i]) = \mathbb{E}_{\varphi \sim p^b(\varphi)} [P_{\varphi}(\mathbf{s}[i] | \mathbf{y}[i])], \quad (6)$$

for each data symbol at $i \in \mathcal{B}^{\text{info}}$. By combining multiple predictions as in (6), with each decision based on a different realization of φ under the optimized distribution $p^b(\varphi)$, Bayesian prediction (6) can account for the uncertainty on the optimal model parameters. This way, it can generally obtain a better calibration performance compared with frequentist learning [24], [25].

D. Model-Based Deep Receivers

The DeepSIC architecture proposed in [12] is a modular model-based DNN-aided MIMO receiver, based on the classic soft interference cancellation (SIC) algorithm [26]. SIC operates in Q iterations, refining an estimate of the conditional probability mass function of each transmitted k^{th} symbol, denoted by $\hat{P}^{(k,q)}$ where q is the iteration number. The estimate is generated for every symbol $k \in \{1, \dots, K\}$ and every iteration $q \in \{1, \dots, Q\}$ by using the soft estimates $\{\hat{P}^{(l,q-1)}\}_{l \neq k}$ of the interfering symbols $\{\mathbf{s}_l\}_{l \neq k}$ obtained in the previous iteration $q-1$ as well as the channel output $\mathbf{y}[i]$. This procedure is illustrated in Fig. 1(a).

In DeepSIC, interference cancellation and soft detection steps are implemented with DNNs. Specifically, the soft estimate of the symbol transmitted by k^{th} user in the q^{th}

Algorithm 2: Bayesian DeepSIC

Input : Channel output \mathbf{y} ; Distribution over entire modules $p^b(\varphi^{\text{SIC}})$; Ensemble size J .
Output: Soft estimations for all users $\{\hat{P}^{(k,Q)}\}_{k=1}^K$.

- 1 **Bayesian Inference**
- 2 **for** $j \in \{1, \dots, J\}$ **do**
- 3 Generate $\varphi_j^{\text{SIC}} \sim p^b(\varphi^{\text{SIC}})$;
- 4 $\{\hat{P}_j^{(k,Q)}\}_{k=1}^K \leftarrow \text{DeepSIC Inference}(\mathbf{y}, \varphi_j^{\text{SIC}})$;
- 5 **return** $\{\frac{1}{J} \sum_{j=1}^J \hat{P}_j^{(k,Q)}\}_{k=1}^K$

iteration is calculated by a DNN-based classifying module with parameter vector $\varphi^{(k,q)}$. Specifically, for a channel output $\mathbf{y}[i]$, we have $K \times 1$ probability mass function vector

$$\hat{P}^{(k,q)}[i] = P_{\varphi^{(k,q)}}(\cdot | \mathbf{y}[i], \{\hat{P}^{(l,q-1)}[i]\}_{l \neq k}). \quad (7)$$

Accordingly, DeepSIC is parameterized by the set of model parameter vectors $\varphi^{\text{SIC}} = \{\{\varphi^{(k,q)}\}_{k=1}^K\}_{q=1}^Q$. The entire DeepSIC architecture is illustrated in Fig. 1(b) and its inference procedure is summarized in Algorithm 1.

In the original reference [12], DeepSIC was trained in a frequentist manner, i.e., by minimizing the cross-entropy loss (3), taking $\prod_{k=1}^K P_{\varphi^{(k,Q)}}(\mathbf{s}_k[i] | \mathbf{y}[i], \{\hat{P}^{(l,Q-1)}[i]\}_{l \neq k})$ in lieu of $P_{\varphi}(\mathbf{s}[i] | \mathbf{y}[i])$. It was shown in [12] that, by predicting information symbols as

$$P_{\varphi^{\text{SIC}}}(\mathbf{s}[i] | \mathbf{y}[i]) = \prod_{k=1}^K P_{\varphi^{(k,Q)}}(\mathbf{s}_k[i] | \mathbf{y}[i], \{\hat{P}^{(l,Q-1)}[i]\}_{l \neq k})$$

for each data symbol at $i \in \mathcal{B}^{\text{info}}$, DeepSIC can outperform frequentist black-box deep receivers under limited pilots scenarios. However, its calibration performance is not discussed.

III. MODULAR MODEL-BASED BAYESIAN LEARNING

Bayesian learning is known to improve the calibration of black-box DNNs models [24], [27]. In this section, we combine Bayesian learning with the modular DeepSIC architecture. To this end, we first present a naïve implementation of Bayesian learning to DeepSIC in Subsection III-A. Then, we introduce the proposed modular model-based Bayesian framework applied to DeepSIC in Subsection III-B.

A. Bayesian DeepSIC

A naïve application of Bayesian training to DeepSIC would proceed as follows. Having obtained the distribution $p^b(\varphi^{\text{SIC}})$ over the set of model parameter vectors φ^{SIC} by minimizing the free energy loss (5), the prediction for information symbols is computed as

$$P_{\varphi^{\text{BSIC}}}(\mathbf{s}[i] | \mathbf{y}[i]) = \mathbb{E}_{\varphi^{\text{SIC}} \sim p^b(\varphi^{\text{SIC}})} [P_{\varphi^{\text{SIC}}}(\mathbf{s}[i] | \mathbf{y}[i])], \quad (8)$$

for each data symbol at $i \in \mathcal{B}^{\text{info}}$, with soft prediction $\hat{P}^{(l,Q-1)}$ following (7). The resulting inference procedure is described in Algorithm 2.

While the final prediction $P_{\varphi^{\text{BSIC}}}(\mathbf{s} | \mathbf{y})$ is obtained by ensembling the predictions of multiple parameter vectors $\varphi^{\text{SIC}} \sim p^b(\varphi^{\text{SIC}})$, the intermediate predictions made during

Algorithm 3: Model-Based Bayesian DeepSIC

Input : Channel output \mathbf{y} ; Distributions per module $\{\{p^{\text{mb}}(\varphi^{(k,q)})\}_{k=1}^K\}_{q=1}^Q$; Ensemble size J .

Output: Soft estimations for all users $\{\hat{P}^{(k,Q)}\}_{k=1}^K$.

1 Model-Based Bayesian Inference

```
2   Generate an initial guess  $\{\hat{P}^{(k,0)}\}_{k=1}^K$ .
3   for  $q \in \{1, \dots, Q\}$  do
4       for  $k \in \{1, \dots, K\}$  do
5           for  $j \in \{1, \dots, J\}$  do
6               Generate  $\varphi_j^{(k,q)} \sim p^{\text{mb}}(\varphi^{(k,q)})$ ;
7                $\hat{P}_j^{(k,q)} = P_{\varphi_j^{(k,q)}}(\cdot | \mathbf{y}, \{\hat{P}^{(l,q-1)}\}_{l \neq k})$ ;
8                $\hat{P}^{(k,q)} = \frac{1}{J} \sum_{j=1}^J \hat{P}_j^{(k,q)}$ ;
9   return  $\{\hat{P}^{(k,Q)}\}_{k=1}^K$ 
```

SIC iterations, i.e., $\hat{P}^{(k,q)}$ with $q < Q$, are computed in a frequentist manner as in (7). Thus, this form of Bayesian learning only encourages the outputs, i.e., the predictions at iteration Q , to be calibrated, not accounting for the internal modular structure of the architecture. The soft estimates learned by the internal modules may still be overconfident, which does not necessarily improve end-to-end accuracy.

B. Modular Model-Based Bayesian DeepSIC

Here, we present a more sophisticated application of Bayesian learning that is tailored to the modular architecture of model-based deep receivers based on DeepSIC. This is achieved by calibrating of the intermediate SIC blocks via Bayesian learning, as detailed next.

Training: During training, we optimize the distribution $p^{\text{mb}}(\varphi^{(k,q)})$ over the parameter vector $\varphi^{(k,q)}$ of each $(k^{\text{th}}, q^{\text{th}})$ block, i.e., $\varphi^{(k,q)} \sim p^{\text{mb}}(\varphi^{(k,q)})$, individually. These distributions are obtained by minimizing the free energy loss on a per-module basis as

$$p^{\text{mb}}(\varphi^{(k,q)}) = \arg \min_{p'} \left(\mathbb{E}_{\varphi^{(k,q)} \sim p'} [\mathcal{L}_{CE}^{\text{MSIC}}(\varphi^{(k,q)})] + \frac{1}{\beta} \text{KL}(p'(\varphi^{(k,q)}) || p^{\text{prior}}(\varphi^{(k,q)})) \right). \quad (9)$$

In (9) the model-based cross-entropy loss function for the parameter vector $\varphi^{(k,q)}$ is defined as

$$\mathcal{L}_{CE}^{\text{MBSIC}}(\varphi^{(k,q)}) = - \sum_{i \in \mathcal{B}^{\text{pilot}}} \log P_{\varphi^{(k,q)}}(\mathbf{s}_k[i] | \mathbf{y}[i], \{\hat{P}^{(l,q-1)}[i]\}_{l \neq k}). \quad (10)$$

Here, the soft estimate $\hat{P}^{(k,q)}[i]$ for k^{th} symbol at the q^{th} iteration is computed by taking into account the uncertainty of the corresponding model parameter vector $\varphi^{(k,q)}$ as

$$\hat{P}^{(k,q)}[i] = \mathbb{E}_{\varphi^{(k,q)} \sim p^{\text{mb}}(\varphi^{(k,q)})} [P_{\varphi^{(k,q)}}(\cdot | \mathbf{y}[i], \{\hat{P}^{(l,q-1)}[i]\}_{l \neq k})].$$

Inference: Having computed a possibly different distribution for the weights of each intermediate module, prediction

of the information symbols is computed as

$$P_{\varphi^{\text{MBSIC}}}(\mathbf{s}[i] | \mathbf{y}[i]) = \prod_{k=1}^K \mathbb{E}_{\varphi^{(k,Q)} \sim p^{\text{mb}}(\varphi^{(k,Q)})} \left[P_{\varphi^{(k,Q)}}(\mathbf{s}_k[i] | \mathbf{y}[i], \{\hat{P}^{(l,Q-1)}[i]\}_{l \neq k}) \right],$$

for each data symbol at $i \in \mathcal{B}^{\text{info}}$. The proposed modular model-based Bayesian inference algorithm for DeepSIC is summarized in Algorithm 3.

IV. NUMERICAL EVALUATIONS

In this section we numerically evaluate the proposed modular model-based Bayesian learning framework by examining the receiver performance in uplink MIMO communications.

Receivers: We evaluate the following MIMO receivers:

- *DNN Detector:* As a benchmark, we use a black-box DNN baseline consisted of three fully connected (FC) layers of sizes $N \times 60$, 60×60 , and $60 \times M^K$, with ReLU activations and a softmax output layer.
- *DeepSIC:* We also consider the conventional DeepSIC as detailed in Subsection II-D with $Q = 2$ iterations, with each DNN-module comprised of two FC layers with hidden layer size 64 and a ReLU activation. We recall that training follows the standard frequentist paradigm.
- *Bayesian DeepSIC:* Bayesian DeepSIC carries out optimization of the distribution $p^{\text{b}}(\varphi)$ in an end-to-end fashion as described in Section III-A.
- *Modular Model-Based Bayesian DeepSIC:* The proposed model-based Bayesian learning introduced in Section III-B that applies Bayesian learning to each module.

For Bayesian learning, i.e., to minimize the free energy loss (5), we adopt the MC dropout scheme [27], [28]. MC dropout parameterizes the distribution $p^{\text{b}}(\varphi)$ in terms of nominal model parameter vector and the dropout probability vector. During Bayesian training, we set the inverse temperature parameter $\beta = 10^2$, and set the ensemble size $J = 5$ during Bayesian inference. For all schemes, optimization is done via Adam with $I = 400$ iterations and learning rate $\eta = 5 \cdot 10^{-3}$. These values were set empirically to ensure convergence¹.

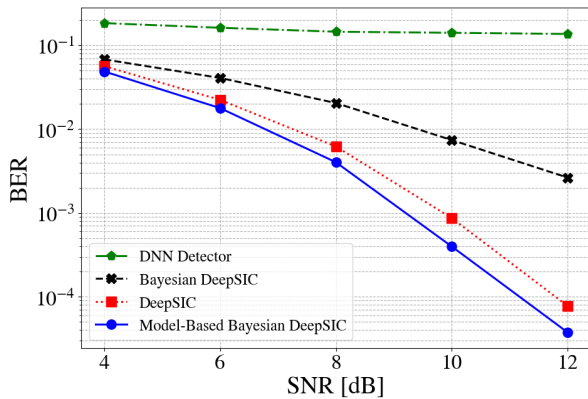
Setup: We transmit 50 blocks, each one composed of $B^{\text{pilot}} = 400$ pilot symbols followed by $B^{\text{info}} = 4 \cdot 10^3$ information symbols. Thus, only a small number of pilots are available to train the DNN-aided receiver. The considered input-output relationship of the memoryless Gaussian MIMO channel is given by

$$\mathbf{y}[i] = \mathbf{H} \mathbf{s}[i] + \mathbf{w}[i], \quad (11)$$

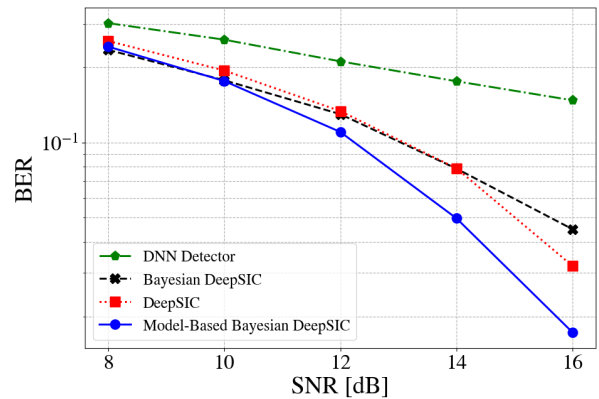
where \mathbf{H} is a fixed $N \times K$ channel matrix, and $\mathbf{w}[i]$ is a complex white Gaussian noise vector. The matrix \mathbf{H} models spatial exponential decay, and its entries are given by $(\mathbf{H})_{n,k} = e^{-|n-k|}$, for each $n \in \{1, \dots, N\}$ and $k \in \{1, \dots, K\}$.

Accuracy: We first evaluate the accuracy of hard detection in terms of BER, i.e., $\mathbb{E}[\mathbb{1}(\hat{\mathbf{s}}[i] \neq \mathbf{s}[i])]$ with $\mathbb{1}(\cdot)$ being the

¹The source code used in our experiments is available at <https://github.com/tomerraviv95/bayesian-learning-for-receivers>



(a) Results for QPSK Constellation.



(b) Results for 8-PSK Constellation.

Fig. 2: BER as a function of SNR for different DNN-aided MIMO receivers. At each block, training is done with 400 pilot symbols and the BER is computed from $4 \cdot 10^3$ information symbols. Results are averaged over 50 blocks.

indicator function. The transmitted symbols are generated in a uniform i.i.d. manner over two different constellations, the first being the quadrature phase shift keying (QPSK) constellation ($\mathcal{S} = \{(\pm \frac{1}{\sqrt{2}}, \pm \frac{1}{\sqrt{2}})\}$) and the second being 8-ary phase shift keying (8-PSK) constellation, i.e., $\mathcal{S} = \{e^{j\frac{\pi\ell}{4}} | \ell \in \{0, \dots, 7\}\}$. Under QPSK, the number of users and antennas are set as $K = N = 5$, while under 8-PSK they are set as $K = N = 3$. The resulting BERs versus SNR are reported in Fig. 2, where the gains of model-based Bayesian learning are apparent as it outperforms all other considered receivers for all SNRs. Specifically, it consistently outperforms DeepSIC by up to 1 dB in the low and high SNR regime for both constellations. In contrast, naïve application of Bayesian learning to DeepSIC seems to harm BER performance, while the black-box DNN struggles to learn from such limited pilots.

Calibration: Next, we investigate the calibration performance of the soft detection. We evaluate two standard measures: (i) reliability diagrams [29] and (ii) expected calibration error (ECE) [10].

A prediction model $P_\varphi(s|\mathbf{y})$ is *perfectly calibrated* if the conditional distribution of the transmitted symbols given the predictor's output satisfies the equality

$$P(s = \hat{s} | P_\varphi(\hat{s}|\mathbf{y}) = \pi) = \pi \text{ for all } \pi \in [0, 1]. \quad (12)$$

In order to measure how close the considered model satisfies the perfect calibration condition (12), reliability diagram first partitions the *confidence level* π into M ranges, i.e., $\{(0, \frac{1}{M}], \dots, (\frac{M-1}{M}, 1]\}$, and define the m^{th} bin as

$$\mathcal{B}_m = \{i \in \mathcal{B}^{\text{info}} : P_\varphi(\hat{s}[i]|\mathbf{y}[i]) \in (\frac{m-1}{M}, \frac{m}{M}]\}.$$

Accordingly, the within-bin accuracy and confidence are respectively computed as

$$\text{Acc}(\mathcal{B}_m) = \frac{1}{|\mathcal{B}_m|} \sum_{i \in \mathcal{B}_m} \mathbb{1}(\hat{s}[i] = s[i]),$$

$$\text{Conf}(\mathcal{B}_m) = \frac{1}{|\mathcal{B}_m|} \sum_{i \in \mathcal{B}_m} P_\varphi(\hat{s}[i]|\mathbf{y}[i]).$$

For perfect calibration (12), the within-bin accuracy $\text{Acc}(\mathcal{B}_m)$ of a well-calibrated predictor should be similar to the within-bin confidence $\text{Conf}(\mathcal{B}_m)$ for every \mathcal{B}_m .

The reliability diagram plots both the within-bin accuracy and confidence as a function of the bin range, as depicted in Fig. 3, for SNR of 10 dB and the 8-PSK constellation (with the number of users and antennas set as before to 3). The bottom part of Fig. 3 shows the number of samples in each \mathcal{B}_m . To guarantee meaningful reliable measures [30], we remove bins with less than 100 samples. As discussed, the original DeepSIC receiver is shown to produce overconfident decisions (Fig. 3(a), red bars are higher than blue bars), while DeepSIC with Bayesian learning has more reliable soft decision outputs as compared to frequentist DeepSIC (Fig. 3(b,c), red bars are similar to blue bars).

In addition to the reliability plot, the ECE is conventionally used as a scalar measure that summarizes the overall calibration performance of the model. The ECE computes the average absolute difference between the within-bin accuracy and within-bin confidence, weighted by the number of samples that lie in each range, and is thus given by [10]

$$\text{ECE} = \sum_{m=1}^M \frac{|\mathcal{B}_m|}{\sum_{m=1}^M |\mathcal{B}_m|} \left(|\text{Acc}(\mathcal{B}_m) - \text{Conf}(\mathcal{B}_m)| \right). \quad (13)$$

The closer the ECE is to zero the more reliable the receiver is. The ECE values reported in Fig. 3 validate the conclusion that our modular model-based Bayesian learning is notably more reliable than frequentist DeepSIC. It also improves upon DeepSIC with naïve application of Bayesian learning, while considerably outperforming it in BER as shown in Fig. 2.

V. CONCLUSION

This paper has introduced modular model-based Bayesian learning, a novel integration of Bayesian learning and modular DNN-based architectures, for wireless receiver design. The proposed approach harnesses the benefits of Bayesian learning in producing well-calibrated soft outputs for each internal module. As a result, modular model-based Bayesian learning

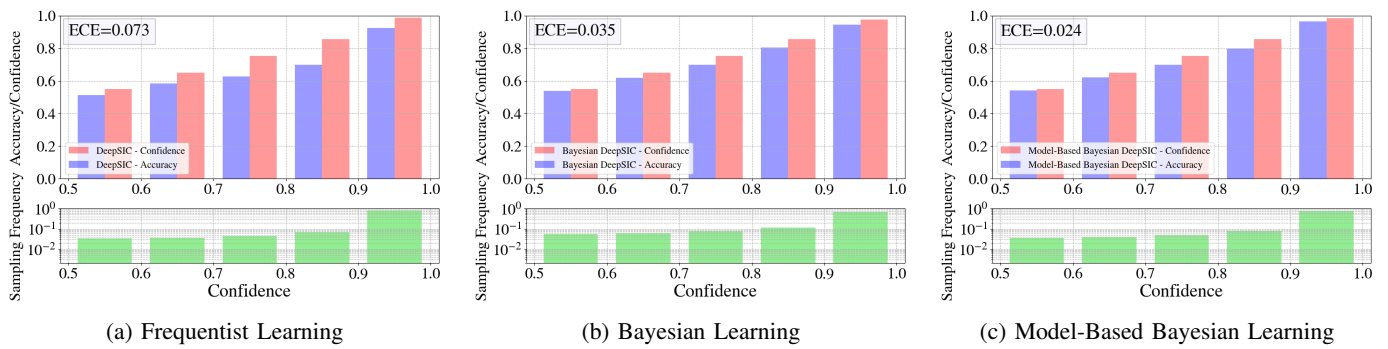


Fig. 3: Reliability diagrams and ECE for (a) original frequentist DeepSIC; (b) naïve application of Bayesian learning to DeepSIC; and (c) model-based Bayesian learning for DeepSIC. Same settings used in Fig. 2 are assumed with fixed SNR of 10 dB and the 8-PSK constellation.

is seen to improve the overall accuracy of DNN-based SIC receivers by mitigating the impact of incorrect, but confident, intermediate decisions made by DNN modules. The accuracy and calibration gains of our framework over conventional frequentist learning and over a naïve output-based application of Bayesian learning come at the cost of additional complexity and latency in the training and inference process, as the reliable soft estimate from each module is obtained from ensembling on a per-module basis. In principle, one can mitigate this issue by employing parallelization, or by sharing distributions among modules. We leave these extensions, along with the investigation of Bayesian learning for other modular architectures, to future work.

REFERENCES

- [1] D. Gündüz, P. de Kerret, N. D. Sidiropoulos, D. Gesbert, C. R. Murthy, and M. van der Schaar, "Machine learning in the air," *IEEE J. Sel. Areas Commun.*, vol. 37, no. 10, pp. 2184–2199, 2019.
- [2] O. Simeone, "A very brief introduction to machine learning with applications to communication systems," *IEEE Trans. on Cogn. Commun. Netw.*, vol. 4, no. 4, pp. 648–664, 2018.
- [3] A. Balatsoukas-Stimming and C. Studer, "Deep unfolding for communications systems: A survey and some new directions," *arXiv preprint arXiv:1906.05774*, 2019.
- [4] N. Farsad, N. Shlezinger, A. J. Goldsmith, and Y. C. Eldar, "Data-driven symbol detection via model-based machine learning," *arXiv preprint arXiv:2002.07806*, 2020.
- [5] Q. Mao, F. Hu, and Q. Hao, "Deep learning for intelligent wireless networks: A comprehensive survey," *IEEE Commun. Surveys Tuts.*, vol. 20, no. 4, pp. 2595–2621, 2018.
- [6] W. Saad, M. Bennis, and M. Chen, "A vision of 6G wireless systems: Applications, trends, technologies, and open research problems," *IEEE Network*, vol. 34, no. 3, pp. 134–142, 2019.
- [7] N. Shlezinger, N. Farsad, Y. C. Eldar, and A. Goldsmith, "Learned factor graphs for inference from stationary time sequences," *IEEE Trans. Signal Process.*, vol. 70, pp. 366–380, 2021.
- [8] Y. Roh, G. Heo, and S. E. Whang, "A survey on data collection for machine learning: a big data-ai integration perspective," *IEEE Trans. Knowl. Data Eng.*, vol. 33, no. 4, pp. 1328–1347, 2019.
- [9] S. T. Jose and O. Simeone, "Free energy minimization: A unified framework for modelling, inference, learning, and optimization," *IEEE Signal Process. Mag.*, vol. 38, no. 2, pp. 120–125, 2021.
- [10] C. Guo, G. Pleiss, Y. Sun, and K. Q. Weinberger, "On calibration of modern neural networks," in *International conference on machine learning*. PMLR, 2017, pp. 1321–1330.
- [11] O. Simeone, *Machine learning for engineers*. Cambridge University Press, 2022.
- [12] N. Shlezinger, R. Fu, and Y. C. Eldar, "DeepSIC: Deep soft interference cancellation for multiuser MIMO detection," *IEEE Trans. Wireless Commun.*, vol. 20, no. 2, pp. 1349–1362, 2021.
- [13] N. Shlezinger, J. Whang, Y. C. Eldar, and A. G. Dimakis, "Model-based deep learning," *arXiv preprint arXiv:2012.08405*, 2020.
- [14] N. Shlezinger, Y. C. Eldar, and S. P. Boyd, "Model-based deep learning: On the intersection of deep learning and optimization," *IEEE Access*, vol. 10, pp. 115 384–115 398, 2022.
- [15] T. Raviv, S. Park, O. Simeone, Y. C. Eldar, and N. Shlezinger, "Online meta-learning for hybrid model-based deep receivers," *IEEE Trans. Wireless Commun.*, 2023, early access.
- [16] N. Shlezinger, N. Farsad, Y. C. Eldar, and A. J. Goldsmith, "Data-driven factor graphs for deep symbol detection," in *2020 IEEE International Symposium on Information Theory (ISIT)*. IEEE, 2020, pp. 2682–2687.
- [17] N. Shlezinger, N. Farsad, Y. C. Eldar, and A. Goldsmith, "Viterbinet: A deep learning based Viterbi algorithm for symbol detection," *IEEE Transactions on Wireless Communications*, vol. 19, no. 5, pp. 3319–3331, 2020.
- [18] T. Raviv, N. Raviv, and Y. Be'ery, "Data-driven ensembles for deep and hard-decision hybrid decoding," in *Proc. IEEE ISIT*, 2020, pp. 321–326.
- [19] T. Van Luong, N. Shlezinger, C. Xu, T. M. Hoang, Y. C. Eldar, and L. Hanzo, "Deep learning based successive interference cancellation for the non-orthogonal downlink," *IEEE Trans. Veh. Technol.*, vol. 71, no. 11, pp. 11 876–11 888, 2022.
- [20] P. Jiang *et al.*, "AI-aided online adaptive OFDM receiver: Design and experimental results," *IEEE Trans. Wireless Commun.*, vol. 20, no. 11, pp. 7655–7668, 2021.
- [21] L. V. Jospin, H. Laga, F. Boussaid, W. Buntine, and M. Bennamoun, "Hands-on Bayesian neural networks—a tutorial for deep learning users," *IEEE Comput. Intell. Mag.*, vol. 17, no. 2, pp. 29–48, 2022.
- [22] D. T. Chang, "Bayesian neural networks: Essentials," *arXiv preprint arXiv:2106.13594*, 2021.
- [23] H. Wang and D.-Y. Yeung, "A survey on Bayesian deep learning," *ACM Computing Surveys (CSUR)*, vol. 53, no. 5, pp. 1–37, 2020.
- [24] M. Zecchin, S. Park, O. Simeone, M. Kountouris, and D. Gesbert, "Robust Bayesian learning for reliable wireless AI: Framework and applications," *arXiv preprint arXiv:2207.00300*, 2022.
- [25] K. M. Cohen, S. Park, O. Simeone, and S. Shamai, "Bayesian active meta-learning for reliable and efficient AI-based demodulation," *IEEE Trans. Signal Process.*, vol. 70, pp. 5366–5380, 2022.
- [26] W.-J. Choi, K.-W. Cheong, and J. M. Cioffi, "Iterative soft interference cancellation for multiple antenna systems," in *Proc. IEEE WCNC*, 2000.
- [27] Y. Gal and Z. Ghahramani, "Dropout as a Bayesian approximation: Representing model uncertainty in deep learning," in *international conference on machine learning*. PMLR, 2016, pp. 1050–1059.
- [28] S. Boluki, R. Ardywibowo, S. Z. Dadaneh, M. Zhou, and X. Qian, "Learnable Bernoulli dropout for Bayesian deep learning," in *International Conference on Artificial Intelligence and Statistics*. PMLR, 2020, pp. 3905–3916.
- [29] M. H. DeGroot and S. E. Fienberg, "The comparison and evaluation of forecasters," *Journal of the Royal Statistical Society: Series D (The Statistician)*, vol. 32, no. 1–2, pp. 12–22, 1983.
- [30] A. Kumar, P. S. Liang, and T. Ma, "Verified uncertainty calibration," *Advances in Neural Information Processing Systems*, vol. 32, 2019.